



You have downloaded a document from
RE-BUŚ
repository of the University of Silesia in Katowice

Title: Unconventional superconductivity in iron-based superconductors in a three-band model

Author: Dawid Crivelli, Andrzej Ptak

Citation style: Crivelli Dawid, Ptak Andrzej. (2014). Unconventional superconductivity in iron-based superconductors in a three-band model. "Acta Physica Polonica. A" (Vol. 126, nr 4A (2014), s. A16-A19), doi 10.12693/APhysPolA.126.A-16



Uznanie autorstwa - Użycie niekomercyjne - Bez utworów zależnych Polska - Licencja ta zezwala na rozpowszechnianie, przedstawianie i wykonywanie utworu jedynie w celach niekomercyjnych oraz pod warunkiem zachowania go w oryginalnej postaci (nie tworzenia utworów zależnych).

Unconventional Superconductivity in Iron-Based Superconductors in a Three-Band Model

D. CRIVELLI AND A. PTOK*

Institute of Physics, University of Silesia, 40-007 Katowice, Poland

Iron-based superconductors exhibit features of systems where the Fulde–Ferrell–Larkin–Ovchinnikov phase, a superconducting state with non-zero total momentum of the Cooper pairs, is actively sought. Experimental and theoretical evidence points strongly to the Fulde–Ferrell–Larkin–Ovchinnikov phase in these materials above the Pauli limit. In this article we discuss the ground state of iron-based superconductors near the critical magnetic field and the full h - T phase diagram for pnictides in case of intra-band pairing, in a three-band model with s_{\pm} symmetry.

DOI: [10.12693/APhysPolA.126.A-16](https://doi.org/10.12693/APhysPolA.126.A-16)

PACS: 74.20.Rp, 74.70.Xa, 74.25.Dw

1. Introduction

In '60s of the XX century, two independent groups, Fulde–Ferrell (FF) [1] and Larkin–Ovchinnikov (LO) [2], proposed a superconducting phase with oscillating order parameter (OP) in real space. This phase, nowadays called the Fulde–Ferrell–Larkin–Ovchinnikov (FFLO) phase, is more stable than the BCS phase in low temperature and hight magnetic field regime. FF proposed a superconducting phase with one momentum \mathbf{q} possible for the Cooper pairs, whereas LO assumed the possibility of two opposite momenta $\pm\mathbf{q}$ — in this case the OP in real space is proportional to $\exp(i\mathbf{q}\cdot\mathbf{r})$ or $\cos(\mathbf{q}\cdot\mathbf{r})$ respectively. A non-zero total momentum of the Cooper pairs bears as a consequence the change of sign of the OP in real space and breaks the spatial symmetry of the system (this is true not only in systems with translation symmetry, but also when rotational symmetry is present [3–5]).

The FFLO phase can be expected in materials with relatively high Maki parameter $\alpha \sim H_{c2}^{\text{orb}}/H_{c2}^P$, when the orbital critical magnetic field H_{c2}^{orb} is greater than the paramagnetic critical field H_{c2}^P . Therefore a good class of candidate to find the FFLO are heavy fermions materials (such as CeCoIn₅) [6–12], organic superconductors [13] and quantum gases [14]. The FFLO phase can exist also in inhomogeneous systems in presence of impurities [15–17] or spin density waves [18]. Moreover, these inhomogeneities can increase the tendency system to create the FFLO phase and stabilize it in a lower magnetic field [17, 19]. The FFLO phase can be also stabilized by pair hopping interaction [20, 21] or in system with nonstandard quasiparticles with spin-dependent mass [22–24].

Other good candidates to find the FFLO phase are iron-based superconductors (IBSC) [25–29] — the characteristic feature of these chemical compounds are

iron–arsenide layers (Fig. 1a), which imply multi-band properties such as the characteristic Fermi surface (with hole- and electron-like Fermi pockets around the $(0,0)$ and (π,π) point respectively, illustrated in Fig. 1b) [30–32]. IBSC are materials with high Maki parameter and anisotropic upper magnetic fields [33–40]. Experimentally a phase transition inside the superconducting state has been observed, which can be evidenced about the phase transition from convectional superconductivity to the FFLO phase [41]. These results are in agreement with theoretical expectations [29, 42, 43].

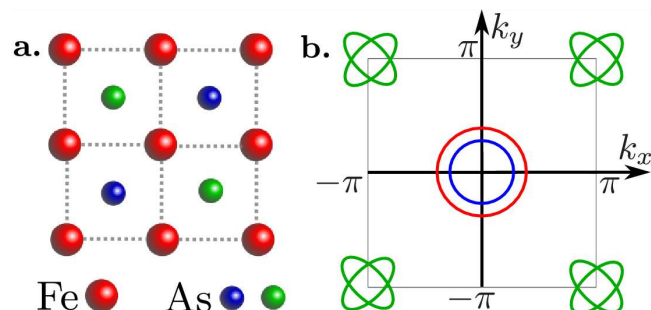


Fig. 1. (a) FeAs layer in iron-based superconductors. Fe (red dot) and As (blue and green dots) ions form a quadratic lattice. As ions are placed above (blue) or under (green) the centers of the squares formed by Fe. (b) True Fermi surface in first Brillouin zone, for two Fe ions per unit cell.

In this paper we analyze IBSC (pnictides) using the three band model proposed by Daghofer et al. [44, 45]. In Sect. 2 we describe details of theoretical calculation, in Sect. 3 we show and discuss numerical results. We summarize the results in Sect. 4. Parameters for the model are listed in Appendix (Sect. 5).

2. Theoretical part

The general Hamiltonian for the multi-orbital system can be written as $H = H_0 + H_I$. The non-interacting part H_0 is given by

*corresponding author; e-mail: aptok@mimj.pl

$$H_0 = \sum_{\mathbf{k}\sigma,\alpha\beta} \left(T_{\mathbf{k}}^{\alpha\beta} - (\mu + \sigma h) \Delta_{\alpha\beta} \right) c_{\mathbf{k}\alpha\sigma}^\dagger c_{\mathbf{k}\beta\sigma}, \quad (1)$$

where $c_{\mathbf{k}\alpha\sigma}^\dagger (c_{\mathbf{k}\alpha\sigma})$ is the creation (annihilation) operator for a spin σ electron of momentum \mathbf{k} in the orbital α . Hopping matrix elements $T_{\mathbf{k}}^{\alpha\beta}$ are given by the effective tight-binding model of the two-dimensional FeAs planes in the given model (see Appendix). Integer α and β label the orbitals. Band structure of the FeAs system can be reconstructed by diagonalization of the Hamiltonian H_0 :

$$H'_0 = \sum_{\mathbf{k}\varepsilon\sigma} E_{\mathbf{k}\varepsilon\sigma} d_{\mathbf{k}\varepsilon\sigma}^\dagger d_{\mathbf{k}\varepsilon\sigma}. \quad (2)$$

μ is the chemical potential, changing the average number of particles in the system $n = \frac{1}{N} \sum_{\mathbf{k}\alpha\sigma} c_{\mathbf{k}\alpha\sigma}^\dagger c_{\mathbf{k}\alpha\sigma} = \frac{1}{N} \sum_{\mathbf{k}\alpha\sigma} d_{\mathbf{k}\alpha\sigma}^\dagger d_{\mathbf{k}\alpha\sigma}$, where N is the number of lattice site. h is the external magnetic field parallel to lattice. ε labels the bands.

We introduce a superconducting pairing between quasi-particles in bands ε . In absence of interband pairing or when it is weak [46], we can effectively describe superconductivity in the FFLO phase by the Hamiltonian

$$H'_{\text{SC}} = \sum_{\varepsilon\mathbf{k}} \left(\Delta_{\varepsilon\mathbf{k}} d_{\varepsilon\mathbf{k}\uparrow}^\dagger d_{\varepsilon,-\mathbf{k}+\mathbf{q}_\varepsilon\downarrow}^\dagger + \text{H.c.} \right), \quad (3)$$

where $\Delta_{\varepsilon\mathbf{k}} = \Delta_\varepsilon \eta(\mathbf{k})$ is the amplitude of the OP for the Cooper pairs with total momentum \mathbf{q}_ε . The structure factor is given by $\eta(\mathbf{k}) = 4 \cos(k_x) \cos(k_y)$ for s_{\pm} -wave symmetry of the OP [28]. As we see, in case of intra-band pairing we have formally an n -band system described by the total Hamiltonian $H = H'_0 + H'_{\text{SC}}$, with n independent bands ε . Using the Bogoliubov transformation we can find a final fermions basis $\Gamma_{\varepsilon\mathbf{k}} = (\gamma_{\varepsilon\mathbf{k}\uparrow}, \gamma_{\varepsilon,-\mathbf{k}\downarrow})^T$, describing the quasi-particle excitation in the superconducting state

$$H = \sum_{\varepsilon\mathbf{k}\tau} \bar{E}_{\varepsilon\mathbf{k}\tau} \gamma_{\varepsilon\mathbf{k}\tau}^\dagger \gamma_{\varepsilon\mathbf{k}\tau} + \text{const} \quad (4)$$

with

$$\begin{aligned} \bar{E}_{\varepsilon\mathbf{k}\tau} &= \frac{E_{\varepsilon\mathbf{k}\uparrow} - E_{\varepsilon,-\mathbf{k}+\mathbf{q}\downarrow}}{2} \\ &+ \tau \sqrt{\left(\frac{E_{\varepsilon\mathbf{k}\uparrow} + E_{\varepsilon,-\mathbf{k}+\mathbf{q}\downarrow}}{2} \right)^2 + |\Delta_{\varepsilon\mathbf{k}}|^2} \end{aligned} \quad (5)$$

where $\tau = \pm$. Total free energy is given by $\Omega = \sum_\varepsilon \Omega_\varepsilon$, where

$$\begin{aligned} \Omega_\varepsilon &= -k_B T \sum_{\mathbf{k}\tau} \ln (1 + \exp(-\beta \bar{E}_{\varepsilon\mathbf{k}\tau})) \\ &+ \sum_{\mathbf{k}} \left(E_{\varepsilon\mathbf{k}\downarrow} - \frac{|\Delta_{\varepsilon\mathbf{k}}|^2}{V_\varepsilon} \right) \end{aligned} \quad (6)$$

is the free energy in band ε in the presence of effective interaction intensity V_ε . The ground state for fixed h and T can be found by minimizing the free energy with respect to the OPs.

3. Numerical results

Numerical calculations were carried out for a square lattice $N_X \times N_Y = 2000 \times 2000$ with periodic boundary conditions. First, the effective pairing intra-band potential V_ε has been determined for every band, in case of s_{\pm} symmetry of the order parameter — to find its value we seek the disappearance of the superconducting BCS phase in each band at the same critical magnetic field $h_C^{\text{BCS}} = 0.005$ eV (and temperature $k_B T = 10^{-5}$ eV). Secondly, we determine the h - T phase diagram for those fixed values.

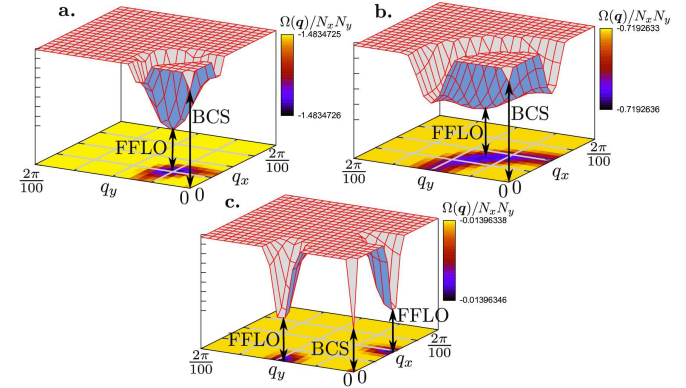


Fig. 2. The free energy per site $\Omega_\varepsilon(\mathbf{q})/N_x N_y$ for s_{\pm} symmetry, for different values of the Cooper pair momentum \mathbf{q} , showing the location of the minima and indicating the existence of different phases. Results for $h \simeq 0.005$ eV = h_C^{BCS} and temperature $k_B T = 10^{-5}$ eV.

3.1. Ground state at the BCS critical magnetic field

To determine the h - T phase diagram with V_ε fixed, we vary the total momentum of the Cooper pairs \mathbf{q} to find the ground state. Results for magnetic field $h \sim h_C^{\text{BCS}}$ and temperature $k_B T = 10^{-5}$ eV are shown in Fig. 2. As we see for every band and $\mathbf{q} = 0$, there exists a local minimum of the free energy $\Omega_\varepsilon(\mathbf{q})$ corresponding to the BCS phase. However, we find the true ground state by the global minimum, which is attained for $\mathbf{q} \neq 0$. For the first two bands ($\varepsilon = 1, 2$ — parts (a) and (b), respectively) the ground state can be found for four equivalent total momenta $\mathbf{q}_{1,2}$ in directions $[1, \pm 1]$. In the third band ($\varepsilon = 3$ — part (c)) the global minimum also exists at non-zero total momentum of the Cooper pairs, but in direction $[0, 1]$ or $[1, 0]$. This result is in agreement with other theoretical results for pnictides in a minimal two-band model [28, 29] and one-band heavy fermions systems [12, 19, 21 (first paper), 47], where the FFLO phase exhibits precisely this direction of the momentum.

3.2. Phase diagram h - T

For fixed values of the effective pairing potential V_ε , we find the h - T phase diagram for each band, as shown in Fig. 3. The region of the BCS phase on the phase diagram

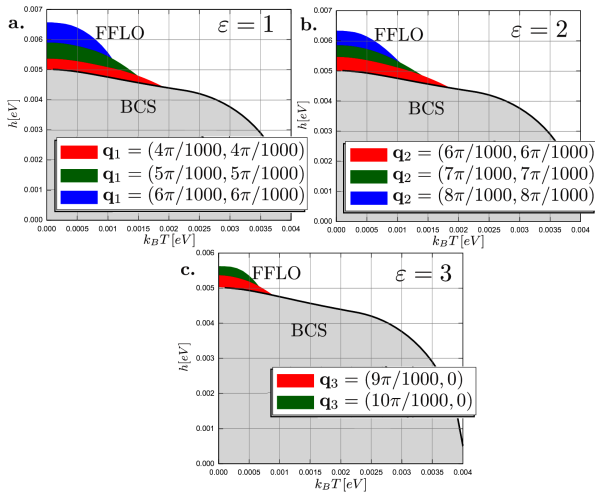


Fig. 3. $h - T$ phase diagram for given effective pairing potential V_ε . Grey area shows region of existing BCS phase. Lines mark the phase transitions. Colors (red, green and blue) mark the regions of the FFLO phase with different values of the total momentum of the Cooper pairs \mathbf{q}_ε .

has a typical form. Above the critical magnetic field for BCS phase and at low temperatures, the FFLO phase can form (cyan region in Fig. 3). In the first two bands, the critical magnetic field of the FFLO phase is bigger than in the third band (Fig. 3) — for the chosen values of V_ε this difference is approximately equal to $\frac{1}{5}h_C^{\text{BCS}}$.

3.3. Total momentum of the Cooper pairs

Minimization of the free energy gives the total momentum of the Cooper pairs (shown in Fig. 2 in magnetic field near h_C^{BCS}). Its value $|\mathbf{q}_\varepsilon|$ is higher for the first band than for the second and third bands. However an increase in the magnetic field raises the total momentum magnitude (red, green and blue areas in Fig. 3), as in the IBSC two-band model [29].

In every band the critical magnetic fields of the phase transition from the FFLO phase to normal state $h_C^{\text{FFLO}}(T)$ are different. Consequence of this are the observed multiple transitions inside the FFLO area of the phase diagram, associated with changes in the modules of total momentum of the Cooper pairs $|\mathbf{q}_\varepsilon|$. Moreover this leads to amplitude modulation of the order parameter in real space, in agreement with the results in the two-band case [29, 42, 43]. To observe this feature would be an experimental check of the existence of the FFLO phase in these materials [41], since we expect more than one phase transition to exist, associated with disappearance of the FFLO phase in selected bands when increasing the external magnetic field h .

4. Summary

Using the three-band model proposed by Daghofer et al. [44, 45] we make a case for the FFLO phase in iron-

based superconductors in presence of intra-band pairing with s_{\pm} -wave symmetry. As in previous theoretical works [28, 29] we show that the ground state of pnictides, above the critical magnetic field of BCS phase and in low temperature, is an unconventional superconductor of the FFLO type. The full phase diagram has been obtained on lattices of thermodynamically relevant sizes, marking the typical area of the BCS phase and how the FFLO can be found beyond its borders, in regimes detrimental to the existence of BCS superconductivity. Consequence of this is the amplitude modulation of the order parameter in real space and multiple phase transitions, in agreement with the literature [29, 42, 43].

Appendix Three-orbital model Daghofer et al. [44]

This model of IBSC was proposed by Daghofer et al. in Ref. [44] and improved in Ref. [45]. Beyond d_{xz} and d_{yz} orbitals the model also accounts for d_{xy} orbital

$$\begin{aligned} T_{\mathbf{k}}^{11} &= 2t_2 \cos k_x + 2t_1 \cos k_y + 4t_3 \cos k_x \cos k_y \quad (\text{A1}) \\ &+ 2t_{11}(\cos(2k_x) - \cos(2k_y)) + 4t_{12} \cos(2k_x) \cos(2k_y), \end{aligned}$$

$$\begin{aligned} T_{\mathbf{k}}^{22} &= 2t_1 \cos k_x + 2t_2 \cos k_y + 4t_3 \cos k_x \cos k_y \quad (\text{A2}) \\ &- 2t_{11}(\cos(2k_x) - \cos(2k_y)) + 4t_{12} \cos(2k_x) \cos(2k_y), \end{aligned}$$

$$\begin{aligned} T_{\mathbf{k}}^{33} &= \epsilon_0 + 2t_5(\cos k_x + \cos k_y) + 4t_6 \cos k_x \cos k_y \\ &+ 2t_9(\cos(2k_x) + \cos(2k_y)) \\ &+ 4t_{10}(\cos(2k_x) \cos k_y + \cos k_x \cos(2k_y)), \quad (\text{A3}) \end{aligned}$$

$$T_{\mathbf{k}}^{12} = T_{\mathbf{k}}^{21} = 4t_4 \sin k_x \sin k_y, \quad (\text{A4})$$

$$T_{\mathbf{k}}^{13} = \bar{T}_{\mathbf{k}}^{31} = 2it_7 \sin k_x + 4it_8 \sin k_x \cos k_y, \quad (\text{A5})$$

$$T_{\mathbf{k}}^{23} = \bar{T}_{\mathbf{k}}^{32} = 2it_7 \sin k_y + 4it_8 \sin k_y \cos k_x. \quad (\text{A6})$$

In Ref. [45] the hopping parameters in electron volts are given as: $t_1 = -0.08$, $t_2 = 0.1825$, $t_3 = 0.08375$, $t_4 = -0.03$, $t_5 = 0.15$, $t_6 = 0.15$, $t_7 = -0.12$, $t_8 = 0.06$, $t_9 = 0.0$, $t_{10} = -0.024$, $t_{11} = -0.01$, $t_{12} = 0.0275$ and $\epsilon_0 = 0.75$. Average number of particles in the system $n = 4$ is attained for $\mu = 0.4748$.

Acknowledgments

D.C. acknowledges support by the FORSZT Ph.D. fellowship.

References

- [1] P. Fulde, R.A. Ferrell, *Phys. Rev.* **135**, A550 (1964).
- [2] A.I. Larkin, Yu.N. Ovchinnikov, *Zh. Eksp. Teor. Fiz.* **47**, 1136 (1964); *Sov. Phys. JETP* **20**, 762 (1965).
- [3] Y. Yanase, *Phys. Rev. B* **80**, 220510 (R) (2009).
- [4] M. Iskin, C.J. Williams, *Phys. Rev. A* **78**, 011603 (R) (2008).
- [5] A. Ptok, *J. Supercond. Nov. Magn.* **25**, 1843 (2012).

- [6] C. Capan, A. Bianchi, R. Movshovich, A.D. Christianson, A. Malinowski, M.F. Hundley, A. Lacerda, P.G. Pagliuso, J.L. Sarrao, *Phys. Rev. B* **70**, 134513 (2004).
- [7] C.F. Micela, M. Nicklas, D. Parker, K. Maki, J.L. Sarrao, J.D. Thompson, G. Sparn, F. Steglich, *Phys. Rev. Lett.* **96**, 117001 (2006).
- [8] A. Bianchi, R. Movshovich, C. Capan, P. G. Pagliuso, J. L. Sarrao, *Phys. Rev. Lett.* **91**, 187004 (2003).
- [9] C. Martin, C.C. Agosta, S.W. Tozer, H.A. Radovan, E.C. Palm, T.P. Murphy, J.L. Sarrao, *Phys. Rev. B* **71**, 020503 (2005).
- [10] V.F. Correa, T.P. Murphy, C. Martin, K.M. Purcell, E.C. Palm, G.M. Schmiedeshoff, J.C. Cooley, S.W. Tozer, *Phys. Rev. Lett.* **98**, 087001 (2007).
- [11] K. Kakuyanagi, M. Saitoh, K. Kumagai, S. Takashima, M. Nohara, H. Takagi, Y. Matsuda, *Phys. Rev. Lett.* **94**, 047602 (2005).
- [12] Y. Matsuda, H. Shimahara, *J. Phys. Soc. Jpn.* **76**, 051005 (2007).
- [13] R. Lortz, Y. Wang, A. Demuer, P.H.M. Böttger, B. Bergk, G. Zwicknagl, Y. Nakazawa, J. Wosnitza, *Phys. Rev. Lett.* **99**, 187002 (2007).
- [14] R. Casalbuoni, G. Nardulli, *Rev. Mod. Phys.* **76**, 263 (2004).
- [15] Q. Wang, C.R. Hu, C.S. Ting, *Phys. Rev. B* **74**, 212501 (2006).
- [16] Q. Wang, C.R. Hu, C.S. Ting, *Phys. Rev. B* **75**, 184515 (2007).
- [17] A. Ptok, *Acta Phys. Pol. A* **118**, 420 (2010).
- [18] A. Ptok, M.M. Maśka, M. Mierzejewski, *Phys. Rev. B* **84**, 094526 (2011).
- [19] M. Mierzejewski, A. Ptok, M.M. Maśka, *Phys. Rev. B* **80**, 174525 (2010).
- [20] A. Ptok, M. Mierzejewski, *Acta Phys. Pol. A* **114**, 209 (2008).
- [21] A. Ptok, M.M. Maśka, M. Mierzejewski, *J. Phys. Condens. Matter* **21**, 295601 (2009); K. Kapcia, S. Robaszkiewicz, R. Micnas, *J. Phys. Condens. Matter* **24**, 215601 (2012); K. Kapcia, S. Robaszkiewicz, *J. Phys. Condens. Matter* **25**, 065603 (2013).
- [22] J. Kaczmarczyk, J. Jędrak, J. Spałek, *Acta Phys. Pol. A* **118**, 261 (2010).
- [23] J. Kaczmarczyk, J. Spałek, *J. Phys. Cond. Matter* **22**, 355702 (2010).
- [24] M.M. Maśka, M. Mierzejewski, J. Kaczmarczyk, J. Spałek, *Phys. Rev. B* **82**, 054509 (2010).
- [25] Y. Kamihara, T. Watanabe, M. Hirano, H. Hosono, *J. Am. Chem. Soc.* **130**, 3296 (2008).
- [26] A. Gurevich, *Phys. Rev. B* **82**, 184504 (2010).
- [27] A. Gurevich, *Rep. Prog. Phys.* **74**, 124501 (2011).
- [28] A. Ptok, D. Crivelli, *J. Low Temp. Phys.* **172**, 226 (2013).
- [29] A. Ptok, *Eur. Phys. J. B* **87**, 2 (2014).
- [30] D.J. Singh, M.H. Du, *Phys. Rev. Lett.* **100**, 237003 (2008).
- [31] H. Ding, P. Richard, K. Nakayama, K. Sugawara, T. Arakane, Y. Sekiba, A. Takayama, S. Souma, T. Sato, T. Takahashi, Z. Wang, X. Dai, Z. Fang, G.F. Chen, J.L. Luo, N.L. Wang, *Europhys. Lett.* **83**, 47001 (2008).
- [32] T. Kondo, A.F. Santander-Syro, O. Copie, Ch. Liu, M.E. Tillman, E.D. Mun, J. Schmalian, S.L. Bud'ko, M.A. Tanatar, P.C. Canfield, A. Kaminski, *Phys. Rev. Lett.* **101**, 147003 (2008).
- [33] G. Fuchs, S.L. Drechsler, N. Kozlova, G. Behr, A. Köhler, J. Werner, K. Nenkov, R. Klingeler, J. Hamann-Borrero, C. Hess, A. Kondrat, M. Grobosch, A. Narduzzo, M. Knupfer, J. Freudenberger, B. Büchner, L. Schultz, *Phys. Rev. Lett.* **101**, 237003 (2008).
- [34] T. Terashima, M. Kimata, H. Satsukawa, A. Harada, K. Hazama, S. Uji, H. Harima, G.F. Chen, J.L. Luo, N.L. Wang, *J. Phys. Soc. Jpn.* **78**, 063702 (2009).
- [35] N. Kurita, K. Kitagawa, K. Matsubayashi, A. Kismarahardja, E.S. Choi, J.S. Brooks, Y. Uwamoto, S. Uji, T. Terashima, *J. Phys. Soc. Jpn.* **80**, 013706 (2011).
- [36] K. Cho, H. Kim, M.A. Tanatar, Y.J. Song, Y.S. Kwon, W.A. Coniglio, C.C. Agosta, A. Gurevich, R. Prozorov, *Phys. Rev. B* **83**, 060502(R) (2011).
- [37] J.L. Zhang, L. Jiao, F.F. Balakirev, X.C. Wang, C.Q. Jin, H. Q. Yuan, *Phys. Rev. B* **83**, 174506 (2011).
- [38] S. Khim, B. Lee, J.W. Kim, E.S. Choi, G.R. Stewart, K.H. Kim, *Phys. Rev. B* **84**, 104502 (2011).
- [39] Y. Liu, M.A. Tanatar, V.G. Kogan, H. Kim, T.A. Lograsso, R. Prozorov, *Phys. Rev. B* **87**, 134513 (2013).
- [40] P. Burger, F. Hardy, D. Aoki, A.E. Böhmer, R. Eder, R. Heid, T. Wolf, P. Schweiss, R. Fromknecht, M.J. Jackson, C. Paulsen, C. Meingast, *Phys. Rev. B* **88**, 014517 (2013).
- [41] D.A. Zocco, K. Grube, F. Eilers, T. Wolf, H. v. Löhneysen, *Phys. Rev. Lett.* **111**, 057007 (2013).
- [42] T. Mizushima, M. Takahashi, K. Machida, *J. Phys. Soc. Jpn.* **83**, 023703 (2014).
- [43] M. Takahashi, T. Mizushima, K. Machida, *Phys. Rev. B* **89**, 064505 (2014).
- [44] M. Daghofer, A. Nicholson, A. Moreo, E. Dagotto, *Phys. Rev. B* **81**, 014511 (2010).
- [45] M. Daghofer, A. Nicholson, A. Moreo, *Phys. Rev. B* **85**, 184515 (2012).
- [46] I.I. Mazin, *Nature* **464**, 183 (2010).